ELSEVIER

Journal of Organometallic Chemistry 654 (2002) 150–161

Journal of Organometallic Chemistry

www.elsevier.com/locate/jorganchem

# Chemistry of Rh(I) complexes based on mesogenic 3,5-disubstituted pyrazole ligands. X-ray crystal structures of 3,5-di(4-*n*-butoxyphenyl)pyrazole ($Hpz^{bp2}$) and $[Rh(\mu\text{-}pz^{R2})(CO)_2]_2$ ($R = C_6H_4OC_nH_{2n+1}$, $n = 10$, 12) compounds. Part II☆

M.C. Torralba [a], M. Cano [a,*], J.A. Campo [a], J.V. Heras [a], E. Pinilla [a,b], M.R. Torres [b]

[a] *Departamento de Química Inorgánica I, Facultad de Ciencias Químicas, Universidad Complutense, E-28040 Madrid, Spain*
[b] *Laboratorio de Difracción de Rayos-X, Facultad de Ciencias Químicas, Universidad Complutense, E-28040 Madrid, Spain*

Received 22 January 2002; accepted 5 March 2002

**Abstract**

Four new 3,5-disubstituted pyrazoles $Hpz^{R2}$ containing long-chain 4-*n*-alkyloxyphenyl substituents [$R = C_6H_4OC_nH_{2n+1}$; $n = 4$ (**1**), 6 (**2**), 12 (**5**), 14 (**6**)] have been prepared and characterised. All of them showed mesomorphic behaviour, the stability and the range of the mesophases increasing with the length of the chain on the pyrazole. The X-ray structure of $Hpz^{bp2}$ (**1**) showed a highly linear molecular shape. Related results were deduced for the remained $Hpz^{R2}$ and the structural consequences agree with the observed mesomorphic properties. The mesogenic pyrazoles $Hpz^{R2}$ (**1**–**6**) were used as ligands towards $[RhCl(CO)_2]$ and $[Rh(CO)_2]$ fragments. $[RhCl(CO)_2(Hpz^{R2})]$ complexes (**7**–**12**) showed some physical properties dependant on the long-chained pyrazoles, and related to different molecular arrays in the solid state. In all cases these compounds evolved to $[Rh(\mu\text{-}pz^{R2})(CO)_2]_2$ in solution. The pyrazolate Rh(I) complexes $[Rh(\mu\text{-}pz^{R2})(CO)_2]_2$ (**13**–**18**) had the usual boat conformation, as deduced by the crystal structure of two of these derivatives [$n = 10$ (**16**), 12 (**17**)]. The packing arrangement has both layer and columnar characteristics. No mesophases have been detected for any of the Rh(I) complexes. © 2002 Published by Elsevier Science B.V.

*Keywords:* Long-chain 3,5-disubstituted pyrazoles; Mesomorphic behaviour; Rhodium–pyrazole complexes; Rhodium–pyrazolate complexes; X-ray structures

## 1. Introduction

Metallomesogens are an important current research field owing to their potential applications. Consequently, interest in the design of new metal complexes with improved properties has increased [1–3]. In this context, in addition to an appropriate molecular shape, other factors have been analysed in order to achieve mesomorphic behaviour. Low molecular symmetry appears to favour stable mesophases [1]. On the other hand, some metallomesogenic complexes have been described containing mesogenic ligands or metal–metal interactions [1–9], although in other cases these features have not been required to achieve the mesomorphic behaviour [7,10–12].

In the first part of our work, we found two types of Rh···Rh interactions between square-planar $[RhCl(CO)_2(Hpz^R)]$ complexes containing pyrazoles with long-chained substituents at the 3 position [13]. As a continuation of our work in this field and following our interest in liquid crystals based on pyrazole derivatives, we are now investigating new rhodium complexes of the type $[RhCl(CO)_2(Hpz^{R2})]$ with related 3,5-disubstituted pyrazole ligands ($R = C_6H_4OC_nH_{2n+1}$; $n = 4$, 6, 8, 10, 12, 14) (Scheme 1). Two of these pyrazoles with $n = 8$ and 10 have previously been reported as mesogenic compounds [14]. In this work, the mesomorphic behaviour of the other four pyrazoles is described. The designed Rh-complexes $[RhCl(CO)_2(Hpz^{R2})]$, in addition to containing mesogenic ligands, are rod-like unsymmetrical molecules with, potentially, metal–metal

☆ Part I, see Ref. [13].

* Corresponding author. Fax: +34-91-3944352.
*E-mail address:* mmcano@quim.ucm.es (M. Cano).

0022-328X/02/$ - see front matter © 2002 Published by Elsevier Science B.V.
PII: S0022-328X(02)01400-6

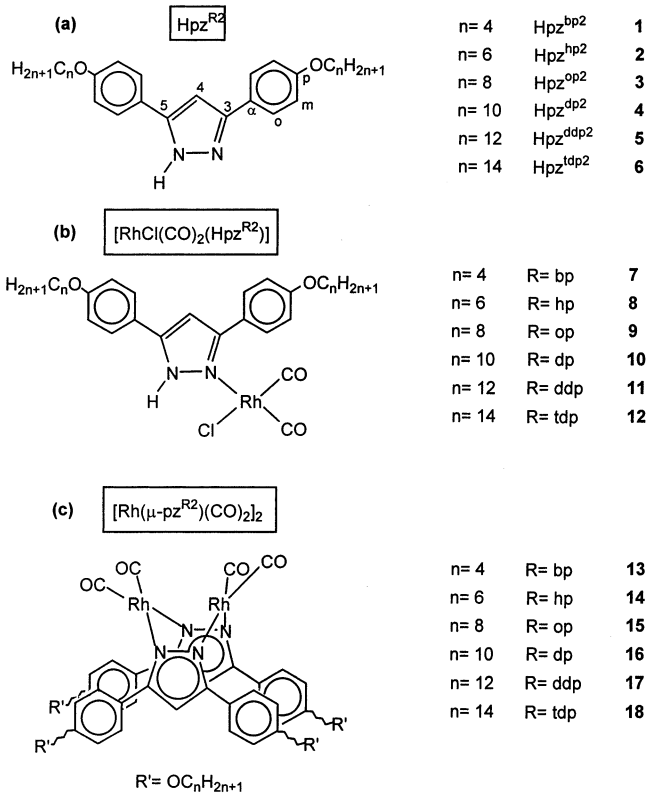


Scheme 1.

interactions. These characteristics make them interesting for investigation of calamitic complexes.

On the other hand, the previously reported X-ray structures of some $[Rh(\mu\text{-}pz^{R})(L_2)]_2$ complexes showed a bowl-shape structure [15–17], which could also be predicted for the related complexes studied in this work. From these derivatives columnar mesophases by stacking of the bowls on top each other could be suggested.

In summary, the aim of this work was to widen the knowledge of structure/mesomorphic properties relationship, firstly, with 3,5-alkyloxyphenyl substituted pyrazole ligands ($Hpz^{R2}$) and, secondly, with their Rh(I) complexes containing $[RhCl(CO)_2]$ or $[Rh(CO)_2]$ fragments. In particular we have investigated the liquid crystal properties of four new pyrazoles $Hpz^{R2}$ [R = $C_6H_4OC_nH_{2n+1}$; $n = 4$ ($Hpz^{bp2}$, **1**), 6 ($Hpz^{hp2}$, **2**), 12 ($Hpz^{ddp2}$, **5**), 14 ($Hpz^{tdp2}$, **6**) (Scheme 1a). These compounds have either shorter and longer chains than those of the related mesogenic pyrazoles with $n = 8$ ($Hpz^{op2}$, **3**) and 10 ($Hpz^{dp2}$, **4**) [14]. The structure of **1** has been solved and the molecular geometry and packing established. The Rh(I) complexes $[RhCl(CO)_2(Hpz^{R2})]$ (R = bp, hp, op, dp, ddp, tdp; **7**–**12**) and $[Rh(\mu\text{-}pz^{R2})(CO)_2]_2$ (R = bp, hp, op, dp, ddp, tdp; **13**–**18**) have also been prepared and characterised (Scheme 1b and c, respectively). Evolution of $[RhCl(CO)_2(Hpz^{R2})]$ to $[Rh(\mu\text{-}pz^{R2})(CO)_2]_2$ prevented adequate crystals for X-ray studies from being obtained. By contrast, the pyrazolate complexes could be crystallised, and the X-ray structures of two of them, $[Rh(\mu\text{-}pz^{R2})(CO)_2]_2$ (R = dp, **16**; ddp, **17**), have been solved. Both cases had the presence of the expected $Rh(\mu\text{-}pz)_2Rh$ boat core, with four long linear alkyloxy chains in an almost parallel disposition.

The mesomorphic behaviour of both pyrazole ligands and Rh-complexes, $[RhCl(CO)_2(Hpz^{R2})]$ and $[Rh(\mu\text{-}pz^{R2})(CO)_2]_2$, was investigated by differential scanning calorimetry (DSC) and polarising light microscopy. Unfortunately non-mesomorphic behaviour was found for both types of Rh-complexes, although $[Rh(\mu\text{-}pz^{R2})(CO)_2]_2$ appear to have ordered phases close to the melting point.

## 2. Experimental

### 2.1. Materials and physical measurements

All commercial reagents were used as supplied. The starting Rh-complex $[Rh(\mu\text{-}Cl)(CO)_2]_2$ was purchased from Sigma–Aldrich and used as supplied.

The 4-*n*-alkyloxyacetophenone and ethyl 4-*n*-alkyloxybenzoate derivatives were synthesised by alkylation of 4-hydroxyacetophenone or ethyl 4-hydroxybenzoate, respectively with the corresponding *n*-alkyliodide in $C_3H_6O$ solution of $K_2CO_3$ as previously described for related compounds [13,18,19]. All these compounds were characterised satisfactorily by analytical and spectroscopic techniques.

Elemental analyses for carbon, hydrogen and nitrogen were carried out by the Microanalytical Service of the Complutense University. IR spectra were recorded on a FTIR Nicolet Magna-550 spectrophotometer with samples as KBr pellets or in $CH_2Cl_2$ solution in the 4000–400 $cm^{-1}$ region. The IR spectra in the 400–200 $cm^{-1}$ region were recorded on a Perkin–Elmer 1300 spectrometer using KBr pellets.

$^1H$- and $^{13}C\{^1H\}$-NMR spectra were performed on a Varian VXR-300 or on a Bruker AM-300 spectrophotometers of the NMR Service of the Complutense University on $CDCl_3$ solutions. Chemical shifts $\delta$ are listed in ppm relative to $Me_4Si$ using the signal of the deuterated solvent as reference, and coupling constants *J* are in hertz. Multiplicities are indicated as s (singlet), d (doublet), t (triplet), qt (quintuplet), st (sextuplet), m (multiplet) and br s (broad signal). The atomic numbering used in the assignment of the NMR signals is shown in Scheme 1. The $^1H$ and $^{13}C$ chemical shifts are accurate to 0.01 and 0.1 ppm, respectively, and coupling constants are accurate to 0.3 Hz for $^1H$-NMR spectra.

Phase studies were carried out by optical microscopy using an Olympus BX50 microscope equipped with a Linkam THMS 600 heating stage. The temperatures

were assigned on the basis of optic observations with polarised light.

Measurements of the transition temperatures were made using a Perkin–Elmer Pyris 1 differential scanning calorimeter with the sample (2–6 mg) hermetically sealed in aluminium pans and with a heating or cooling rate of 5–10° $min^{-1}$.

### 2.2. Synthetic methods

#### 2.2.1. Preparation of $Hpz^{R2}$ (R = bp **1**, hp **2**, ddp **5**, tdp **6**)

To a mixture of 4-*n*-alkyloxyacetophenone (20 mmol) and ethyl 4-*n*-alkyloxybenzoate (30 mmol) in dimethoxyethane (80 ml) was carefully added 60% NaH (50 mmol), and then the mixture refluxed for 3 h. The mixture was cooled at room temperature (r.t.), poured in water (150 ml) and acidified with dilute HCl. The product was extracted several times with $Et_2O$, and the combined extracts dried over $Na_2SO_4$ and then filtered. Evaporation of the solvent gave the corresponding 1,3-bis(4-*n*-alkyloxyphenyl)propane-1,3-dione which were fully characterised (Yield: ca. 75%).

To a suspension of the β-diketone (2 mmol) in EtOH (50 ml) was added an excess of hydrazine hydrate (2.2 mmol), and the mixture refluxed for 3 h. Then, the solution was allowed to cool at r.t. and kept overnight at 4 °C. The precipitated product was filtered and dried in vacuo, giving rise to the desired pyrazole. Yields are given in Table 1.

#### 2.2.2. Preparation of $[RhCl(CO)_2(Hpz^{R2})]$ (R = bp, hp, op, dp, ddp, tdp) (**7–12**)

To a solution of $[Rh(\mu\text{-}Cl)(CO)_2]_2$ (0.15 mmol) in $CH_2Cl_2$ (2 ml) was added a $CH_2Cl_2$ solution (8 ml) of the corresponding pyrazole $Hpz^{R2}$ (0.30 mmol). The yellow solution was stirred for 1 h under dinitrogen, and then the volume was reduced in vacuo to ca. 2 ml. Addition of $C_6H_{14}$ precipitated a yellow solid. This was filtered off, washed with $C_6H_{14}$ and dried in vacuo. Yields are given in Table 2.

#### 2.2.3. Preparation of $[Rh(\mu\text{-}pz^{R2})(CO)_2]_2$ (R = bp, hp, op, dp, ddp, tdp) (**13–18**)

To a solution of $[Rh(\mu\text{-}Cl)(CO_2)]_2$ (0.15 mmol) in MeOH (2 ml) was added a MeOH slurry (15 ml) of the corresponding pyrazole $Hpz^{R2}$ (0.30 mmol). After few minutes a solution of KOH in MeOH was slowly added and a yellow solid started to precipitate. The mixture was stirred for 1 h and the solid obtained was filtered off, washed with MeOH and dried in vacuo. Yields are given in Table 3.

### 2.3. X-ray structure determination

Colourless prismatic single crystals of $Hpz^{bp2}$ (**1**) were obtained by layering a $CH_2Cl_2$ solution with $Et_2O$. Yellow crystals of $[Rh(\mu\text{-}pz^{R2})(CO)_2]_2$ (R = dp **16**, ddp **17**) were obtained by layering $CH_2Cl_2$ solutions with $C_6H_{14}$. The data were collected on a Enraf–Nonius CAD4, on a Nonius-Kappa CCD and on a Smart Bruker CCD diffractometers for **1**, **16** and **17**, respectively. A summary of the fundamental crystal data for the three compounds is given in Table 4.

The molecular structures were solved by direct methods and conventional Fourier techniques and refined by full-matrix least-squares on $F^2$ [20]. Final mixed refinements were performed for the three compounds with the following differences. For **1**, all non-hydrogen atoms have been refined anisotropically except the carbon atoms in the butoxy chains which were refined isotropically with geometrical restraints. The hydrogen atoms were calculated and refined as riding on the carbon bonded atom with a common isotropic displacement parameter, except H1 bonded to N1 which has been found as the first peak in a Fourier difference, included and its coordinates fixed.

Because no resolvable thermal and positional disorder has been found for **16** and **17**, some carbon atoms in the decyloxy and dodecyloxy chains, respectively, were refined only two cycles anisotropically and in the last cycles the thermal factors have been fixed. These carbon atoms were refined with geometrical restraints and a variable common carbon–carbon distance. The rest of the non-hydrogen atoms were refined anisotropically.

Table 1
IR data, isolated yield and elemental analyses of $Hpz^{R2}$ (R = bp **1**, hp **2**, ddp **5**, tdp **6**) [a]

| Compound | IR [b] ($cm^{-1}$) | | Yield (%) | Molecular formula | Calculated (%) | | | Found (%) | | |
|---|---|---|---|---|---|---|---|---|---|---|
| | ν(NH) | ν(CN) | | | C | H | N | C | H | N |
| **1** | 3229 | 1617 | 85 | $C_{23}H_{28}N_2O_2$ | 75.8 | 7.7 | 7.7 | 75.6 | 8.1 | 7.7 |
| **2** | 3219 | 1615 | 54 | $C_{27}H_{36}N_2O_2$ | 77.2 | 8.6 | 6.7 | 76.9 | 8.9 | 6.4 |
| **5** | 3430 | 1614 | 52 | $C_{39}H_{60}N_2O_2$ | 79.6 | 10.2 | 4.8 | 79.3 | 10.2 | 4.7 |
| **6** | 3431 | 1615 | 76 | $C_{43}H_{68}N_2O_2$ | 80.1 | 10.6 | 4.4 | 79.3 | 10.6 | 4.2 |

[a] Compounds **3** (R = op) and **4** (R = dp) have previously been described [14].
[b] In KBr discs.

Table 2
IR data, colour, isolated yield and elemental analyses of $[RhCl(CO)_2(Hpz^{R2})]$ (R = bp, hp, op, dp, ddp, tdp) (**7**–**12**)

| Compound | IR [a] ($cm^{-1}$) | | | Colour | Yield (%) | Molecular formula | Calculated (%) | | | Found (%) | | |
|---|---|---|---|---|---|---|---|---|---|---|---|---|
| | $\nu$(NH) | $\nu$(CN) | $\nu$(CO) | | | | C | H | N | C | H | N |
| **7** | 3216, 3147 | 1613 | 2081br, 2014br | Deep-yellow | 62 | $C_{25}H_{28}ClN_2O_4Rh$ | 53.7 | 5.1 | 5.0 | 53.7 | 5.0 | 5.0 |
| **8** | 3172, 3141 | 1611 | 2086, 2072, 2015, 2009 | Deep-yellow | 73 | $C_{29}H_{36}ClN_2O_4Rh$ | 56.6 | 5.9 | 4.6 | 56.4 | 5.9 | 4.5 |
| **9** | 3273 | 1613 | 2081, 2003 | Light-yellow | 88 | $C_{33}H_{44}ClN_2O_4Rh$ | 59.1 | 6.6 | 4.2 | 58.7 | 6.6 | 4.1 |
| **10** | 3277 | 1616 | 2082, 2004 | Light-yellow | 64 | $C_{37}H_{52}ClN_2O_4Rh$ | 61.1 | 7.2 | 3.9 | 60.8 | 7.2 | 3.8 |
| **11** | 3275 | 1615 | 2082, 2004 | Light-yellow | 67 | $C_{41}H_{60}ClN_2O_4Rh$ | 62.9 | 7.7 | 3.6 | 62.8 | 7.7 | 3.6 |
| **12** | 3275 | 1614 | 2083, 2004 | Light-yellow | 92 | $C_{45}H_{68}ClN_2O_4Rh$ | 64.4 | 8.2 | 3.3 | 64.2 | 8.1 | 3.3 |

[a] In KBr discs.

The hydrogen atoms were calculated and refined as riding on the carbon bonded atom with a common isotropic displacement parameters.

The largest residual peak in the final difference map was 0.266, 2.95 (at 1.1 Å of the C67 atom) and 0.45 e $Å^{-3}$ for **1**, **16** and **17,** respectively.

## 3. Results and discussion

### 3.1. Ligands $Hpz^{R2}$ (R = bp **1**, hp **2**, ddp **5**, tdp **6**)

The 3,5-di(4-*n*-octyloxyphenyl)pyrazole (**3**) and 3,5-di(4-*n*-decyloxyphenyl)pyrazole (**4**) derivatives have previously been reported as mesogenic compounds [14]. In this work, we have extended this study to new derivatives with either shorter or longer chains. We have synthesised and characterised four new derivatives with $OC_nH_{2n+1}$ chains [$n = 4$ ($Hpz^{bp2}$, **1**), 6 ($Hpz^{hp2}$, **2**), 12 ($Hpz^{ddp2}$, **5**), 14 ($Hpz^{tdp2}$, **6**)] (Scheme 1a) and their mesomorphic behaviour has been studied.

The ligands were prepared by an analogous procedure to that reported for related pyrazoles [13,16,21], and fully characterised by spectroscopic and analytical techniques (Tables 1, 5 and 6). Assignment of the NMR signals was made following the literature precedents [13,16,22,23].

All four derivatives showed enantiotropic mesophases when they were analysed by DSC and polarising light microscopy. The transition temperatures and enthalpies are shown in Table 7. All the pyrazoles except **1** showed more than one mesophase. DSC thermograms of **1** and **5** are depicted in Fig. 1 as representative examples. Textures of the mesophases observed with a polarising light microscope for the same derivatives are shown in Fig. 2. The two most interesting results deal with: (a) the mesophase range; and (b) the melting and clearing points, being wider and lower, respectively with increasing carbon chain length (22.3, 184 and 206.3° for **1** and 60, 116.1 and 160.6° for **6**; see Table 7).

### 3.2. X-ray structure of 3,5-di(4-n-butoxyphenyl)pyrazole $Hpz^{bp2}$ (**1**)

The most favourable geometry for calamitic (rodlike) mesophases is the linear one, and in agreement with this feature we have observed these mesophases in all the pyrazoles investigated.

As structural diffraction data have not been reported for pyrazoles of this type, we were interested in solving the crystal structure of some of these compounds. Then the X-ray structure of $Hpz^{bp2}$ (**1**) has been solved (Fig. 3). This compound crystallises in the $P2_1/n$ space group with four molecules per unity cell. Some representative bond distances and angles are listed in Table 8.

The most interesting feature was the presence of a strong NH···N intermolecular hydrogen bond between the NH group and the N atom of neighbouring molecules (Fig. 4). It suggests a dimeric structure which

Table 3
IR data, colour, isolated yield and elemental analyses of $[Rh(\mu\text{-}pz^{R2})(CO)_2]_2$ (R = bp, hp, op, dp, ddp, tdp) (**13**–**18**)

| Compound | IR [a] ($cm^{-1}$) | | Colour | Yield (%) | Molecular formula | Calculated (%) | | | Found (%) | | |
|---|---|---|---|---|---|---|---|---|---|---|---|
| | $\nu$(CN) | $\nu$(CO) | | | | C | H | N | C | H | N |
| **13** | 1613 | 2087, 2069, 2015 | Yellow | 81 | $C_{50}H_{54}N_4O_8Rh_2$ | 57.5 | 5.2 | 5.4 | 57.6 | 4.8 | 5.4 |
| **14** | 1613 | 2087, 2067, 2015 | Yellow | 71 | $C_{58}H_{70}N_4O_8Rh_2$ | 60.2 | 6.1 | 4.8 | 59.8 | 6.2 | 4.8 |
| **15** | 1613 | 2086, 2068, 2014 | Yellow | 79 | $C_{66}H_{86}N_4O_8Rh_2$ | 62.4 | 6.8 | 4.4 | 60.0 | 6.4 | 4.4 |
| **16** | 1613 | 2086, 2068, 2014 | Yellow | 51 | $C_{74}H_{102}N_4O_8Rh_2$ | 64.3 | 7.4 | 4.1 | 64.3 | 7.5 | 3.9 |
| **17** | 1613 | 2086, 2068, 2014 | Yellow | 76 | $C_{82}H_{118}N_4O_8Rh_2$ | 65.9 | 8.0 | 3.8 | 65.1 | 7.6 | 3.8 |
| **18** | 1613 | 2086, 2068, 2013 | Yellow | 55 | $C_{90}H_{134}N_4O_8Rh_2$ | 67.3 | 8.4 | 3.5 | 66.9 | 8.1 | 3.6 |

[a] In KBr discs.

Table 4
Crystal and refinement data for $Hpz^{bp2}$ (**1**) and $[Rh(\mu\text{-}pz^{R2})(CO)_2]_2$ (R = dp **16**, ddp **17**)

| | **1** | **16** | **17** |
|---|---|---|---|
| Empirical formula | $C_{23}H_{28}N_2O_2$ | $C_{74}H_{102}N_4O_8Rh_2$ | $C_{82}H_{118}N_4O_8Rh_2$ |
| Formula weight | 364.47 | 1381.42 | 1493.62 |
| $T$ (K) | 293(2) | 293(2) | 296(2) |
| Crystal system | Monoclinic | Triclinic | Triclinic |
| Space group | $P2_1/n$ | $P\bar{1}$ | $P\bar{1}$ |
| $a$ (Å) | 15.842(3) | 14.972(1) | 15.106(1) |
| $b$ (Å) | 5.732(2) | 15.491(1) | 16.401(1) |
| $c$ (Å) | 23.976(3) | 17.512(1) | 17.759(1) |
| $\alpha$ (°) | | 79.86(1) | 80.997(2) |
| $\beta$ (°) | 106.66(3) | 74.31(1) | 73.357(2) |
| $\gamma$ (°) | | 67.24(1) | 74.508(2) |
| $V$ (Å$^3$) | 2085.9(9) | 3594.0(4) | 4052.6(6) |
| $Z$ | 4 | 2 | 2 |
| $F(000)$ | 784 | 1456 | 1584 |
| $\rho_{calc}$ (g cm$^{-3}$) | 1.161 | 1.277 | 1.224 |
| $\mu$ (mm$^{-1}$) | 0.074 | 0.514 | 0.461 |
| Crystal dimensions (mm) | 0.40 × 0.15 × 0.12 | 0.20 × 0.20 × 0.15 | 0.20 × 0.17 × 0.12 |
| Scan technique | $\omega/2\theta$ | $\phi$ and $\omega$ | $\phi$ and $\omega$ |
| Data collected | (−18, 0, 0) to (18, 6, 28) | (0, −18, −22) to (19, 20, 23) | (−17, −19, −21) to (9, 18, 20) |
| $\theta$ range (°) | 1.81–24.97 | 1.51–28.32 | 1.20–25.00 |
| Reflections collected | 3590 | 17 781 | 21 440 |
| Independent reflections | 3502 [$R_{int} = 0.017$] | 17 781 | 14 073 [$R_{int} = 0.079$] |
| Data/restraints/parameters | 3502/6/206 | 17 781/44/683 | 14 073/44/541 |
| Observed reflections [$I > 2\sigma(I)$] | 935 | 13 253 | 3838 |
| $R$ [a] | 0.073 | 0.066 | 0.066 |
| $Rw_F$ [b] | 0.289 | 0.179 | 0.185 |

[a] $\Sigma\ [|F_o| - |F_c|]/\ \Sigma\ |F_o|$.
[b] $(\Sigma\ [w(F_o^2 - F_o^2)^2]/\Sigma\ [w(F_o^2)^2])^{1/2}$.

certainly should favour the molecular ordering in the fluid phases [14].

In addition the molecule presents an almost linear geometry which can be deduced from the $\alpha$ angle, as defined in Fig. 5 (Table 9). The $\alpha$ value of 154.1° found for **1** agrees with that obtained for 3,5-diphenylpyrazole from AM1 and CNDO/2 calculations [14]. Unfortunately no adequate crystals from the other pyrazoles could be obtained for X-ray purposes. However, some of their $\alpha$ angles could be deduced by extrapolation from the X-ray structures of some of their corresponding complexes, as will be discussed in Section 3.5 (Table 9). As expected, longer chains at the 3 and 5 positions of the pyrazole give rise to high $\alpha$ values increasing the linearity of these compounds. This fact agrees with the stability range found for the mesophases.

### 3.3. Compounds $[RhCl(CO)_2(Hpz^{R2})]$ (R = bp, hp, op, dp, ddp, tdp) (7–12)

Following our previous results on $[RhCl(CO)_2(Hpz^{R})]$ (R = $C_6H_4OC_nH_{2n+1}$ substituent at the 3 position of the pyrazole) [13], we are now investigating related compounds containing the mesogenic 3,5-disubstituted pyrazoles $Hpz^{R2}$. These complexes $[RhCl(CO)_2(Hpz^{R2})]$ (R = bp, hp, op, dp, ddp, tdp; **7**–**12**) (Scheme 1b) were prepared by reaction of the corresponding pyrazole and $[Rh(\mu\text{-}Cl)(CO)_2]_2$ (Scheme 2i) in an analogous procedure to that described with the related 3-substituted pyrazoles [13].

In our previous work on $[RhCl(CO)_2(Hpz^{R})]$ chemistry, two crystalline polymorphs (red and yellow) were isolated depending on the substituents [13]. The yellow form, which consisted in dimeric unities through Cl bridges, was favoured with the longer-chained substituents. By contrast, the red one defined by the stacking of individual square-planar molecules with considerable metal–metal interactions, was the unique polymorph isolated for the shorter chains.

In this work, the new compounds $[RhCl(CO)_2(Hpz^{R2})]$ (R = bp, hp, op, dp, ddp, tdp; **7**–**12**) were isolated as yellow solids and characterised by spectroscopic (IR and NMR) and analytical techniques (Tables 2 and 5). All of them were air-stable. However, **7** rapidly evolves to $[Rh(\mu\text{-}pz^{bp2})(CO)_2]_2$ (**13**), even when it is stored under dinitrogen. This made its isolation and the study of its thermal behaviour difficult.

From the NMR spectra, well-defined signals for all protons were observed in all cases (Table 5), in agreement with the absence of metallotropic equilibrium. The IR spectra in dichloromethane solution showed the two expected $\nu$(CO) bands at ca. 2085 and 2015 cm$^{-1}$,

Table 5
$^1$H-NMR data ($CDCl_3$, 298 K) of the compounds studied in this work [a]

| Compound | Pyrazole | | $-C_6H_4-$ | | $-OR$ | |
|---|---|---|---|---|---|---|
| | NH [b] | H4 | H*o* | H*m* | | |
| **1** | n.o. | 6.68s | 7.63d<br>$J_{om} = 8.5$ | 6.93d | $CH_2$-1′: 4.00t<br>$CH_2$-2′: 1.80qt<br>$CH_2$-3′: 1.51st<br>$CH_3$-4′: 0.99t | $J_{1'2'} = 6.3$<br>$J_{2'3'} = 7.0$<br>$J_{3'4'} = 7.1$ |
| **6** | n.o. | 6.68s | 7.63d<br>$J_{om} = 8.7$ | 6.95d | $CH_2$-1′: 3.99t<br>$CH_2$-2′: 1.80qt<br>$CH_2$-3′–13′: 1.5–1.1m<br>$CH_3$-14′: 0.88t | $J_{1'2'} = 6.6$<br>$J_{2'3'} = 7.1$<br><br>$J_{13'14'} = 6.8$ |
| **7** | 11.65br s | 6.60s | 7.67d<br>7.51d<br>$J_{om} = 8.4$ | 7.02d<br>6.99d | $CH_2$-1′: 4.03m<br>$CH_2$-2′: 1.80qt<br>$CH_2$-3′: 1.53st<br>$CH_3$-4′: 0.99t | $J_{1'2'} = 6.2$<br>$J_{2'3'} = 7.2$<br><br>$J_{3'4'} = 7.2$ |
| **12** | 11.64br s | 6.60s | 7.66d<br>7.51d<br>$J_{om} = 8.4$ | 7.02d<br>6.98d | $CH_2$-1′: 4.01m<br>$CH_2$-2′: 1.81qt<br>$CH_2$-3′–13′: 1.6–1.2m<br>$CH_3$-14′: 0.88t | $J_{1'2'} = 5.9$<br>$J_{2'3'} = 6.8$<br><br>$J_{13'14'} = 6.7$ |
| **13** | | 6.58s | 7.99d<br>$J_{om} = 8.4$ | 7.05d | $CH_2$-1′: 4.08t<br>$CH_2$-2′: 1.85qt<br>$CH_2$-3′: 1.57st<br>$CH_3$-4′: 1.03t | $J_{1'2'} = 6.4$<br>$J_{2'3'} = 7.5$<br><br>$J_{3'4'} = 7.2$ |
| **18** | | 6.57s | 7.99d<br>$J_{om} = 8.6$ | 7.05d | $CH_2$-1′: 4.07t<br>$CH_2$-2′: 1.86qt<br>$CH_2$-3′–13′: 1.5–1.0m<br>$CH_3$-14′: 0.88t | $J_{1'2'} = 6.4$<br>$J_{2'3'} = 7.2$<br><br>$J_{13'14'} = 6.6$ |

[a] As expected, the NMR data of each type of compounds are similar. Therefore, only those of the first and last compounds of each serie are given as representative examples.
[b] n.o., not observed.

typical of mononuclear Rh(I) compounds [16,24]. However, in the solid state the pattern of the $\nu$(CO) bands was different for **7** and **8** with respect to those containing longer chains (**9**–**12**). The former one was consistent with the presence of four bands or two very broad bands for **8** and **7**, respectively, while the later only exhibited two sharp bands (Table 2). These features could be related with the previous observations of $[RhCl(CO)_2(Hpz^R)]$ complexes [13], for which the unidimensional molecular stacking of the red form was disrupt by the longer-chain substituent giving rise to a favourable approach between the molecules of neighbouring columns, and consequently dimeric unities were obtained (yellow form) [13]. Intense colours (red, blue, violet) are characteristic of unidimensional metal–metal interactions [4,13,16,24–26], but by contrast discrete molecular structures are found with light colours [4,13,27–29]. The adoption of either a unidimensional molecular stacking with metal–metal interactions between $[RhCl(CO)_2(Hpz^R)]$ molecules or $[RhCl(CO)_2(Hpz^R)]_2$ dimers by Rh–Cl···Rh interactions between monomers was ascribed to the steric consequences of the chain length [14]. In this context the new derivatives $[RhCl(CO)_2(Hpz^{R2})]$ (**7**–**12**) could be suggested to have structures in the solid state with different molecular arrays, varying from those with a molecular stacking in which the metal–metal interactions, if there are, are very weak (for **7** and **8**, deep yellow) to those with potential dimeric nature (for **9**–**12**, pale yellow).

The $\nu$(NH) band at ca. 3200 $cm^{-1}$ was shifted in all cases at lower frequencies compared to the free ligands, and it appeared at about the same values observed for related $[RhCl(CO)_2(Hpz^R)]$ compounds which had intramolecular NH···Cl hydrogen bonding interactions [13]. These features support the potential presence of related interactions in the complexes described in this work. In agreement with the carbonyl behaviour, compounds **7** and **8** show the lower $\nu$(NH) values compared with those of **9**–**12**.

Table 6
$^{13}C\{^{1}H\}$-NMR data ($CDCl_3$, 298 K) of the pyrazoles $Hpz^{R2}$ and $[Rh(\mu\text{-}pz^{R2})(CO)_2]_2$ [a]

| Compound | CO | Pyrazole carbons | | | $-C_6H_4-$ | | | | −OR |
|---|---|---|---|---|---|---|---|---|---|
| | | C3 | C4 | C5 | C$\alpha$ | C*o* | C*m* | C*p* | |
| **1** | | 148.6 | 98.9 | 148.6 | 124.2 | 126.9 | 114.9 | 159.3 | C1′: 67.9<br>C2′,3′: 31.4, 19.3<br>C4′: 13.9 |
| **6** | | 148.2 | 98.6 | 148.2 | 123.9 | 126.8 | 114.8 | 159.3 | C1′: 68.1<br>C2′–11′: 31.9, 29.7, 29.5, 29.4, 29.3, 26.0, 22.7<br>C14′: 14.1 |
| **13** | 184.5<br>$J_{Rh} = 66.5$ | 155.6 | 103.4 | 155.6 | 126.2 | 129.4 | 114.2 | 159.2 | C1′: 67.7<br>C2′,13′: 31.3, 19.2<br>C4′: 13.8 |
| **18** | 184.5<br>$J_{Rh} = 67.0$ | 155.7 | 103.5 | 155.7 | 126.3 | 129.5 | 114.3 | 159.3 | C1′: 68.1<br>C2′–13′: 31.9, 29.7, 29.5, 29.4, 26.1, 22.7<br>C14′: 14.1 |

[a] As expected, the NMR data of each type of compounds are similar. Therefore, only those of the first and last compounds of each serie are given as representative examples.

In the low frequency region, the $\nu$(Rh–Cl) band at ca. 300 $cm^{-1}$ had same value as those observed in the red or yellow forms of $[RhCl(CO)_2(Hpz^R)]$ derivatives, so that these results could not been used as guide to define the presence of metal–metal interactions or dimeric structures.

Unfortunately, the evolution observed in solution of $[RhCl(CO)_2(Hpz^{R2})]$ to $[Rh(\mu\text{-}pz^{R2})(CO)_2]_2$ prevented us obtaining crystals of **7**–**12** for the X-ray structural characterisation.

Table 7
Phase properties of the pyrazoles $Hpz^{R2}$ (R = bp **1**, hp **2**, ddp **5**, tdp **6**) determined by DSC [a]

| Compound | Transition | $T$ (°) | $\Delta H$ (kJ $mol^{-1}$) |
|---|---|---|---|
| **1** | $Cr_1 \rightarrow Cr_2$ | 93.2 | 5.0 |
| | $Cr_2 \rightarrow SmA$ | 184.0 | 20.2 |
| | $SmA \rightarrow I$ | 206.3 | 4.9 |
| **2** [b] | $Cr_1 \rightarrow Cr_2$ | 47.4 | 19.5 |
| | $Cr_2 \rightarrow SmC$ | 158.5 | 14.7 |
| | $SmC \rightarrow I$ | 198.0 | 5.0 |
| **5** [c] | $Cr_1 \rightarrow Cr_2$ | 93.4 | 51.6 |
| | $Cr_2 \rightarrow SmC$ | 124.8 | 14.1 |
| | $SmC \rightarrow I$ | 174.9 | 8.0 |
| **6** | $Cr_1 \rightarrow Cr_2$ | 85.8 | 1.4 |
| | $Cr_2 \rightarrow SmX$ [d] | 100.6 | 60.9 |
| | $SmX \rightarrow SmC$ | 116.1 | 14.0 |
| | $SmC \rightarrow I$ | 160.6 | 8.3 |

[a] The phase properties of **3** (R = op) and **4** (R = dp) have previously been described [14].
[b] A new mesophase is only observed by polarising light microscopy at ca. 200 °C corresponding to SmA.
[c] A new mesophase is only observed by polarising light microscopy at ca. 174 °C corresponding to N.
[d] Unknown ordered mesophase.

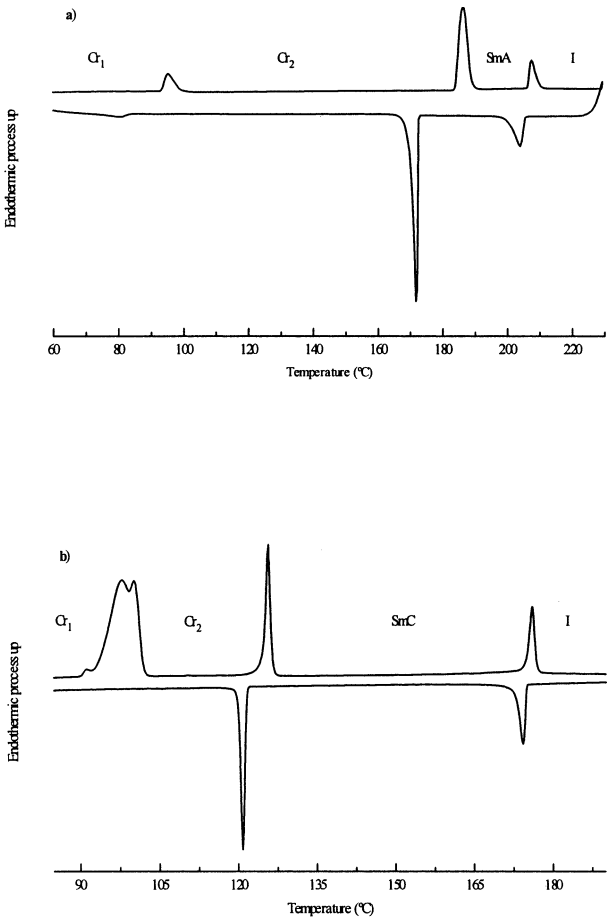


Fig. 1. DSC thermograms of: (a) $Hpz^{bp2}$ (**1**); and (b) $Hpz^{ddp2}$ (**5**).

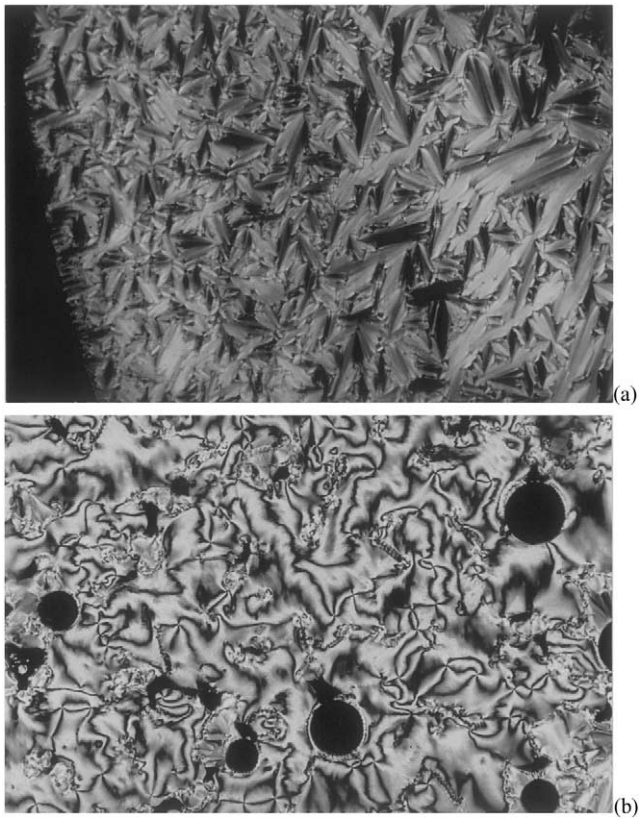


Fig. 2. Textures of the mesophases for: (a) $Hpz^{bp2}$ (**1**) at 204 °C; and (b) $Hpz^{ddp2}$ (**5**) at 170 °C.

Table 8
Selected bond distances (Å) and angles (°) for $Hpz^{bp2}$ (**1**)

| | | | |
|---|---|---|---|
| *Bond distances* | | | |
| N1–N2 | 1.343(6) | C3–C6 | 1.448(8) |
| N1–C5 | 1.358(7) | C5–C12 | 1.446(8) |
| N2–C3 | 1.354(7) | N1–H1 | 0.8639 |
| C3–C4 | 1.390(8) | N2′···H1 | 2.19 |
| C4–C5 | 1.355(7) | N1···N2′ | 2.883(6) |
| *Bond angles* | | | |
| N2–N1–C5 | 112.7(6) | N2–N1–H1 | 119.0 |
| N1–N2–C3 | 105.9(6) | C5–N1–H1 | 128.2 |
| C3–C4–C5 | 109.3(6) | N1–H1···N2′ | 136.9 |

Symmetry operation (′): $-x+2$, $-y+1$, $-z+2$.

### 3.4. Compounds $[Rh(\mu\text{-}pz^{R2})(CO)_2]_2$ ($R$ = bp, hp, op, dp, ddp, tdp) (**13–18**)

In order to obtain adequate crystals of $[RhCl(CO)_2(Hpz^{R2})]$ for X-ray purposes, new products were isolated and determined to be $[Rh(\mu\text{-}pz^{R2})(CO)_2]_2$ (Scheme 2iii) whose identities were confirmed by comparison with IR and NMR spectra of authentic samples (Tables 3, 5 and 6). These complexes were alternatively prepared by reaction of $[Rh(\mu\text{-}Cl)(CO)_2]_2$ and the pyrazolate ligand (Scheme 2ii) in a similar way to that used for the related well-known class of pyrazolate-bridged dimers [15–17].

Complexes **13–18** (Scheme 1c) were isolated as deep yellow solids which were air-stable in the solid state and in solution of various organic solvents. The IR spectra in solid state and in dichloromethane solution have the three expected $\nu$(CO) bands at ca. 2086, 2067 and 2015 $cm^{-1}$ (Table 3). The $^1$H- and $^{13}$C-NMR show the resonances of the pyrazolate groups in the relation corresponding with the proposed formula (Tables 5 and 6). Therefore, only signals due to the equivalence of the four substituents as well as one type for the H(4) and C(4) nuclei were observed.

The formation of $[Rh(\mu\text{-}pz^{R2})(CO)_2]_2$ (**13–18**) through their related monomeric compounds $[RhCl(CO)_2(Hpz^{R2})]$ (**7–12**) is a representative example of the non-requirement of a deprotonating medium (i.e. in apparently neutral conditions) to produce the pyrazolate-bridged coordination. This behaviour has previously been found for other metal-derivatives [30].

### 3.5. X-ray crystal structures of $[Rh(\mu\text{-}pz^{R2})(CO)_2]_2$ ($R$ = dp, **16**; ddp, **17**)

Both complexes are isostructural (space group $P\bar{1}$. The molecular structure of **16** and **17** are illustrated in Figs. 6 and 7 respectively. Selected bond distances and angles with estimated standard deviations are given in Table 10.

Two pyrazolate groups are bonded in an *exo*-bidentate fashion to the two rhodium atoms of the dimer, and two CO groups in each rhodium complete the distorted

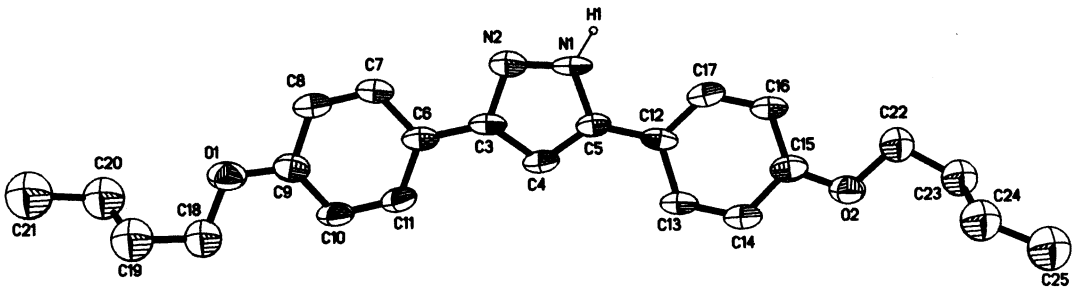


Fig. 3. Perspective ORTEP plot of **1**. Hydrogen atoms, except H1, have been omitted for clarity, and thermal ellipsoids are at 35% probability level.

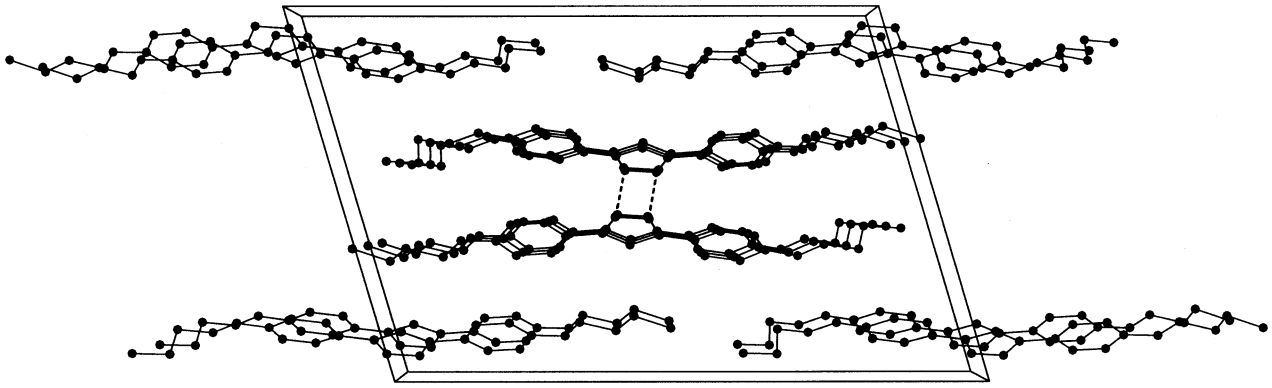

Fig. 4. Molecular packing of **1** through the *b* axis, showing the intermolecular hydrogen bond.

Table 9
Values of the $\alpha$ angle for the pyrazoles $Hpz^{R2}$ (R = bp **1**, dp **4**, ddp **5**) [a]

| Compound | $\alpha$ angle (°) |
|---|---|
| **1** | 154.1 |
| **4** [b] | ~ 162.3 |
| **5** [b] | ~ 164.5 |

[a] $\alpha$ angle as defined in Fig. 5.

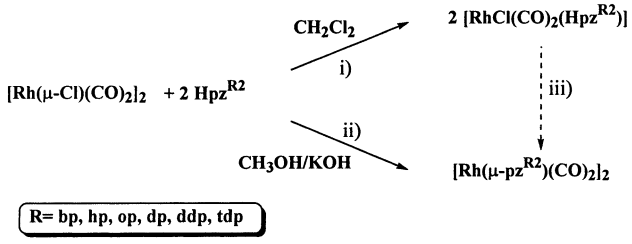


Scheme 2.

square-planar environment. The molecule in both cases comprises a $Rh_2(\mu\text{-pz})_2$ core in which the metallocycle $Rh(NN)_2Rh$ has the usual boat conformation, with the Rh···Rh distance being 3.1633(6) and 3.144(1) Å for **16** and **17**, respectively. Each of the pyrazolate groups carry two terminal alkyloxyphenyl chains in the 3 and 5 positions, and all the aromatic rings in the chains are almost planar. Those phenyl rings at the 5 position (by considering the clockwise direction Rh1N1N2Rh2N4N3) are twisted with respect to their own pyrazolate planes at angles of 36.4(2), 32.9(2)° and 37.6(4), 36.8(4)° for **16** and **17**, respectively, while the other two at the 3 position are more coplanar with their corresponding pyrazolate groups (the corresponding angles are 18.0(2), 24.9(2)° and 18.8(4), 23.0(4)° for **16** and **17**, respectively). The principal molecular axis (which contains both Rh-atoms) could be defined as approximately parallel to the *a* crystallographic axis (angle of 35.13(1) and 35.27(2)° for **16** and **17** respectively).

The packing arrangement can be described as layer-like (Fig. 8). Each layer is formed by the stacking of two sheets of dimers. Each sheet in turn arises from dimers having the same orientation of molecular cores, but opposite between contiguous sheets (i.e. the boats are inverted). Interdigitation between neighbouring molecules of the layer through the long-chained substituents is observed. The layers could be described along a plane (defined by the four nitrogen atoms of the two pyrazolate groups) which forms a dihedral angle of 36.2(2) and 35.7(1)° for **16** and **17** respectively with the plane *ac*.

In addition, by considering the crystallographically imposed molecular disposition, a columnar stacking along the *a* axis could also be defined with interdigitation between substituents of neighbouring columns. However, neither the intermolecular distances in the

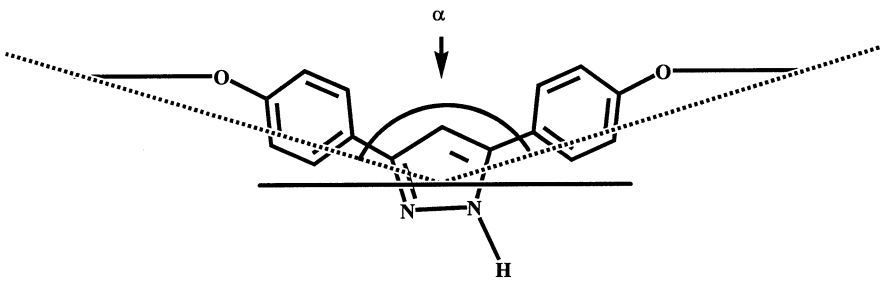


Fig. 5. Schematic representation of the $\alpha$ angle, defined as the angle between the lines connecting the middle of the pyrazole ring and the last carbon of the substituent-chain.

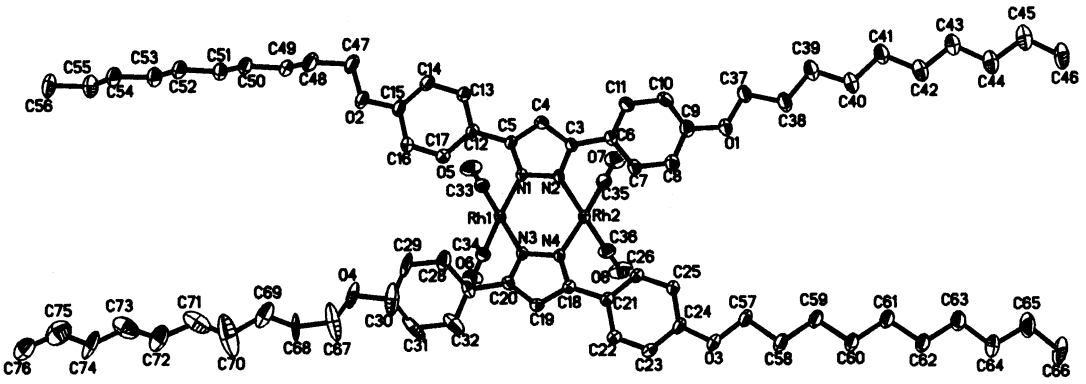


Fig. 6. Perspective ORTEP plot of **16**. Hydrogen atoms have been omitted for clarity, and thermal ellipsoids are at 30% probability level.

Table 10
Selected bond distances (Å) and angles (°) for $[Rh(\mu\text{-}pz^{R2})(CO)_2]_2$ (R = dp **16**, ddp **17**)

| | **16** | **17** |
|---|---|---|
| *Bond distances* | | |
| Rh1···Rh2 | 3.1633(6) | 3.144(1) |
| Rh1–N1 | 2.081(3) | 2.061(8) |
| Rh1–N3 | 2.072(3) | 2.071(7) |
| Rh1–C33 | 1.855(5) | 1.76(1) |
| Rh1–C34 | 1.859(5) | 1.79(1) |
| Rh2–N2 | 2.073(3) | 2.060(7) |
| Rh2–N4 | 2.083(3) | 2.068(8) |
| Rh2–C35 | 1.858(5) | 1.78(1) |
| Rh2–C36 | 1.848(5) | 1.79(1) |
| N1–N2 | 1.377(4) | 1.374(8) |
| N3–N4 | 1.369(4) | 1.382(4) |
| *Bond angles* | | |
| C33–Rh1–C34 | 90.4(2) | 90.7(5) |
| C33–Rh1–N1 | 90.6(2) | 91.8(4) |
| C34–Rh1–N1 | 176.8(2) | 177.1(4) |
| C33–Rh1–N3 | 177.8(2) | 176.2(4) |
| C34–Rh1–N3 | 88.4(2) | 88.2(4) |
| N1–Rh1–N3 | 88.5(1) | 89.2(3) |
| C35–Rh2–C36 | 90.5(2) | 90.2(4) |
| C35–Rh2–N2 | 88.1(2) | 88.8(4) |
| C36–Rh2–N2 | 178.5(2) | 177.7(4) |
| C35–Rh2–N4 | 176.6(2) | 177.1(4) |
| C36–Rh2–N4 | 92.6(2) | 92.6(4) |
| N2–Rh2–N4 | 88.7(1) | 88.4(3) |

column nor the direction of $d_{z^2}$ orbitals of the Rh atoms of the stacked dimers were adequate to render intermolecular interactions.

It is possible that these structural results are related to the lack of a molecular orientation in the fluid phases.

### 3.6. Thermal studies of compounds 7–18

Complexes **7**–**18** have been studied by polarising light microscopy and DSC. The results obtained are summarised in Table 11. No mesophases have been detected for these complexes. However, it is interesting to note that for the pyrazolate Rh-complexes **13**–**18**, some ordering close to the melting point could be proposed from microscopic observations, but unfortunately these transformations could not be detected in the corresponding DSC thermograms. The significant structural changes upon coordination of the mesogenic organic ligands appear to be responsible of the absence of liquid crystal properties on the Rh-complexes. Further efforts should be made to achieve organised liquid phases.

## 4. Supplementary material

Tables of the NMR data of all compounds have been deposited as supplementary material. Crystallographic

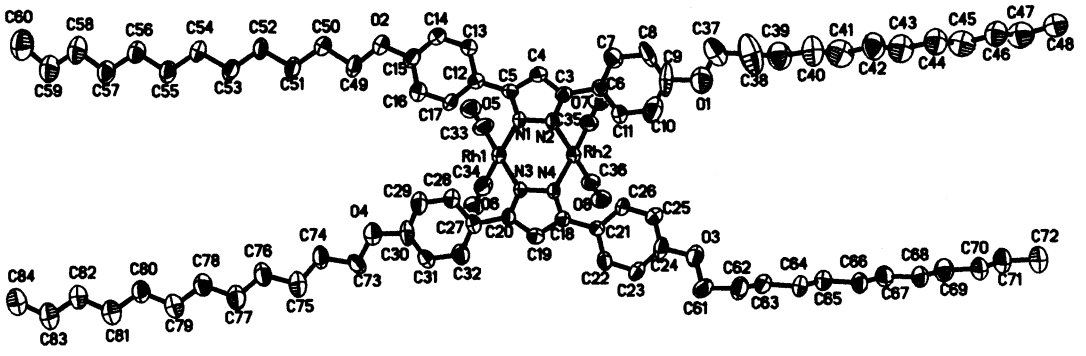


Fig. 7. Perspective ORTEP plot of **17**. Hydrogen atoms have been omitted for clarity, and thermal ellipsoids are at 35% probability level.

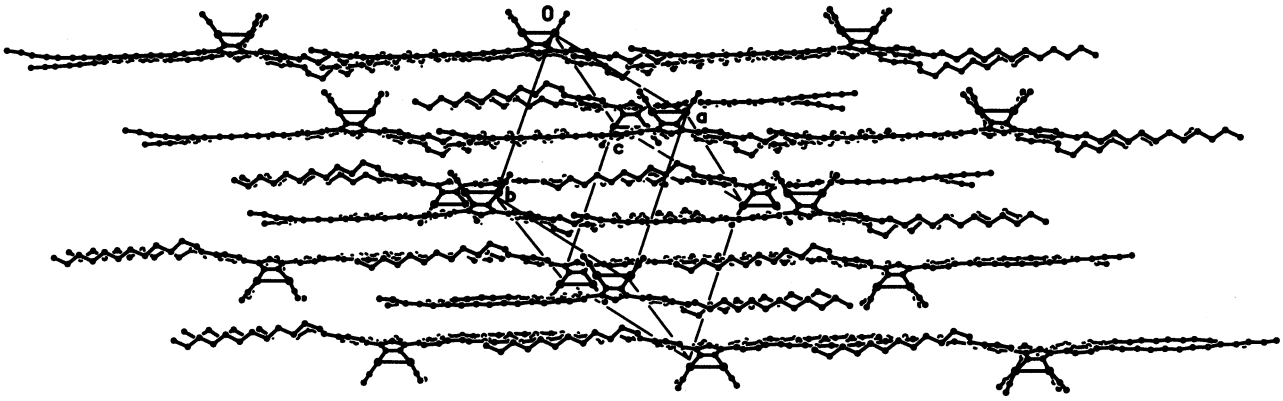


Fig. 8. Molecular arrangement of **17**, showing the layer like distribution. The same distribution is also observed for **16**.

Table 11
Phase properties of compounds **7**–**18** determined by DSC [a]

| Compound | Transition | $T$ (°) | $\Delta H$ (kJ mol$^{-1}$) |
|---|---|---|---|
| **8** | Cr → I | 68.3 | 32.1 |
| **9** | Cr → I | 65.0 | 47.0 |
| **10** | Cr → I | 75.5 | 65.1 |
| **11** | Cr → I | 78.8 | 68.1 |
| **12** | Cr → I | 86.9 | 90.8 |
| **13** | Cr → I | 231.7 | 60.6 |
| **14** | Cr → I | 194.2 | 59.6 |
| **15** | Cr → I | 159.5 | 63.6 |
| **16** | Cr → I | 143.8 | 79.2 |
| **17** | Cr → I | 133.4 | 88.1 |
| **18** | Cr → I | 126.0 | 74.6 |

[a] The unstability of **7** has precluded to study its thermal behaviour.

data for the structural analysis have been deposited with the Cambridge Crystallographic Data Centre, CCDC deposition numbers 176606–176608 for compounds **1**, **16** and **17**. Copies of this information may obtained free of charge from The Director, CCDC, 12 Union Road Cambridge CB2 1EZ, UK (Fax: +44-1223-336033; e-mail: deposit@ccdc.cam.ac.uk or www: http://www.ccdc.cam.ac.uk)

## Acknowledgements

Financial support from the DGES of Spain is gratefully acknowledged (Project no. PB98-0766). We are grateful to Dr A. Coetzee of Nonius (The Netherlands) for the collection of X-ray data of compound **16**.

## References

[1] B. Donnio, D.W. Bruce, Struct. Bond. 95 (1999) 193.
[2] S.R. Collinson, D.W. Bruce, in: J.P. Sauvage (Ed.), Transition Metals in Supramolecular Chemistry (Chapter 7), Wiley, Chichester, 1999, pp. 285–369.
[3] J.L. Serrano (Ed.),Metallomesogens. Synthesis, Properties and Applications, VCH Publishers, New York, 1996.
[4] J. Barberá, A. Elduque, R. Giménez, F.J. Lahoz, J.A. López, L.A. Oro, J.L. Serrano, B. Villacampa, J. Villalba, Inorg. Chem. 38 (1999) 3085.
[5] D.W. Bruce, E. Lalinde, P. Styring, D.A. Dunmur, P.M. Maitlis, J. Chem. Soc. Chem. Commun. (1986) 581.
[6] D.W. Bruce, D.A. Dunmur, M.A. Esteruelas, S.E. Hunt, R. Le Lagadec, P.M. Maitlis, J.R. Marsden, E. Sola, J.M. Stacey, J. Mater. Chem. 1 (1991) 251.
[7] W. Wan, W.J. Guang, K.Q. Zhao, W.Z. Zheng, L.F. Zhang, J. Organomet. Chem. 557 (1998) 157.
[8] P. Berdagué, J. Courtieu, P.M. Maitlis, J. Chem. Soc. Chem. Commun. (1994) 1313.
[9] H. Adams, N.A. Bailey, D.W. Bruce, D.A. Dunmur, E. Lalinde, M. Marcos, C. Ridway, P. Styring, P.M. Maitlis, Liq. Cryst. 2 (1987) 381.
[10] M.A. Esteruelas, E. Sola, L.A. Oro, M.B. Ros, M. Marcos, J.L. Serrano, J. Organomet. Chem. 387 (1990) 103.
[11] H. Adams, N.A. Bailey, D.W. Bruce, S.A. Hudson, J.R. Marsden, Liq. Cryst. 16 (1994) 643.
[12] M.A. Esteruelas, E. Sola, L.A. Oro, M.B. Ros, J.L. Serrano, J. Chem. Soc. Chem. Commun. (1989) 55.
[13] M.C. Torralba, M. Cano, J.A. Campo, J.V. Heras, E. Pinilla, M.R. Torres, J. Organomet. Chem. 633 (2001) 91.
[14] J. Barbera, C. Cativiela, J.L. Serrano, M.M. Zurbano, Liq. Cryst. 11 (1992) 887.
[15] C. López, J.A. Jiménez, R.M. Claramunt, M. Cano, J.V. Heras, J.A. Campo, E. Pinilla, A. Monge, J. Organomet. Chem. 511 (1996) 115.
[16] M. Cano, J.V. Heras, M. Maeso, M. Alvaro, R. Fernández, E. Pinilla, J.A. Campo, A. Monge, J. Organomet. Chem. 534 (1997) 159.
[17] J.A. Campo, M. Cano, J.V. Heras, E. Pinilla, M. Ruiz-Bermejo, R. Torres, J. Organomet. Chem. 582 (1999) 173.
[18] K. Ohta, H. Muroki, K.I. Hatada, I. Yamamoto, K. Matsuzaki, Mol. Cryst. Liq. Cryst. 130 (1985) 249.
[19] J.A. Campo, M. Cano, J.V. Heras, M.C. Lagunas, J. Perles, E. Pinilla, M.R. Torres, Helv. Chim. Acta 84 (2001) 2316.
[20] G.M. Sheldrick, SHELXL97, Program for Refinement of Crystal Structure, University of Göttingen, Göttingen, Germany, 1997.
[21] S. Trofimenko, J.C. Calabrese, J.K. Kochi, S. Wolowiec, F.B. Hulsbergen, J. Reedijk, Inorg. Chem. 31 (1992) 3943.
[22] M. Begtrup, G. Boyer, P. Cabildo, C. Cativiela, R.M. Claramunt, J. Elguero, J.I. García, C. Toiron, P. Vedsø, Magn. Reson. Chem. 31 (1993) 107.
[23] C. López, D. Sanz, R.M. Claramunt, S. Trofimenko, J. Elguero, J. Organomet. Chem. 503 (1995) 265.
[24] M. Cano, J.A. Campo, J.V. Heras, J. Lafuente, C. Rivas, E. Pinilla, Polyhedron 14 (1995) 1139.

[25] M.J. Decker, D.O. Kimberley Fjeldsted, S.R. Stobart, M.J. Zaworotko, J. Chem. Soc. Chem. Commun. (1983) 1525.
[26] G. Aullón, S. Alvarez, Chem. Eur. J. 3 (1997) 655.
[27] G.C. Gordon, P.W. DeHaven, M.C. Weiss, V.L. Goedken, J. Am. Chem. Soc. 100 (1978) 1003.
[28] A. Elduque, C. Finestra, J.A. López, F.J. Lahoz, F. Merchán, L.A. Oro, M.T. Pinillos, Inorg. Chem. 37 (1998) 824.
[29] M.K. Kolel-Veetil, A.L. Rheingold, K.J. Ahmed, Organometallics 12 (1993) 3439.
[30] G. Banditelli, A.L. Bandini, G. Minghetti, F. Bonati, Can. J. Chem. 59 (1981) 1241 (and references therein).